*applied sciences*

MDPI

*Article*

# Optimization of Material and Printing Parameter Selection for FDM 3D-Printed Bone Models for Osteotomy Training: A Biomechanical and User-Based Evaluation

**Moritz Bregenzer [1,2], Yao Li [1,2], Kunpeng Xie [1,2], Leonhard Gerich [1,2], Max Mischer [3], Rainer Röhrig [2], Frank Hölzle [1], Behrus Hinrichs-Puladi [1,2,*,†] and Ashkan Rashad [1,†]**

[1] Department of Oral and Maxillofacial Surgery, University Hospital RWTH Aachen, 52074 Aachen, Germany
[2] Institute of Medical Informatics, University Hospital RWTH Aachen, 52074 Aachen, Germany
[3] Clinic for Orthopaedics, Trauma and Reconstructive Surgery, University Hospital RWTH Aachen, 52074 Aachen, Germany
* Correspondence: bpuladi@ukaachen.de; Tel.: +49-241-80-38389; Fax: +49-241-80-82430
† These authors contributed equally to this work.

### Featured Application

Cost-effective 3D-printed bone models for surgical training in oral and maxillofacial education.

### Abstract

Although additive manufacturing enables cost-effective surgical training models, variation in materials and printing parameters limits standardization. This study combined biomechanical testing and user evaluation to identify fused deposition modeling (FDM) settings for osteotomy simulation. Porcine ribs and three-dimensional (3D)-printed models were compared using three-point bending tests. Subsequently, 32 participants performed osteotomies using an ultrasonic device, a Lindemann bur, and a reciprocating saw. Haptic feedback was assessed by questionnaire, while surface artifacts were evaluated by two blinded evaluators. With 25% gyroid infill and two outer layers, maximum bending forces ranged from 322.9 to 552.1 N across the printed materials, compared with 604.9 N for the porcine ribs, with polylactic acid (PLA) showing the closest approximation. Polycarbonate (PC) achieved the highest haptic rating ($6.7 \pm 1.8$), followed by acrylonitrile styrene acrylate (ASA), polyethylene terephthalate glycol (PETG), and PLA, with a significant difference between PC and PLA ($p = 0.029$). The reciprocating saw received the highest ratings across all criteria. Surface artifacts differed between materials ($p < 0.001$), with PETG and PLA showing more melting and fraying, and ASA and PC more stringing. No significant differences were observed between students and doctors. Overall, PLA most closely approximated the reference maximum bending force, whereas PC and ASA achieved the highest perceived tactile realism.

**Keywords:** 3D printing; fused deposition modeling; osteotomy; surgical training; simulation; additive manufacturing; medical education

Check for updates

Academic Editor: Georgios Romanos

Received: 28 June 2026
Revised: 10 August 2026
Accepted: 18 August 2026
Published: 24 August 2026

**Copyright:** © 2026 by the authors. Licensee MDPI, Basel, Switzerland. This article is an open access article distributed under the terms and conditions of the Creative Commons Attribution (CC BY) license.

## 1. Introduction

Practical surgical training is essential for skill development among students and trainee doctors [1]. In oral and maxillofacial surgery, training is mainly conducted using human or animal cadavers and synthetic models. Soft and hard tissue preparation as well as implantological procedures are described on human cadavers [2], but their routine use is limited

by availability, cost, and ethical considerations [3–5]. Porcine cadavers are commonly used for procedures such as periodontal training [6], whereas synthetic mandibular models are available for implant-placement exercises [7]. Although synthetic models provide a viable alternative, they can be expensive and offer limited anatomical variability [8].

Three-dimensional (3D)-printed bone models provide a promising alternative for training, surgical planning, and simulation [9–11]. They have been used for student training in oral surgery [12], for planning procedures involving complex anatomy such as orbital floor reconstructions [13] and for simulating procedures such as sinus augmentation [14]. Patient-specific 3D-printed anatomical models enhance the understanding of complex anatomical structures [6] and may reduce surgical time by up to 20% while reducing the risk of errors [15–17].

The cost of 3D printers has decreased, making them more affordable and accessible. This has enabled hospitals and training centers to produce these models within a few hours and at minimal cost [18]. The customization of 3D printing makes it particularly valuable in surgical training, as the models can be tailored to reflect specific clinical cases. 3D-printed mandibular models can be embedded in phantom heads to create a more realistic training environment [12]. Compared with cadaveric specimens, printed models also involve fewer storage requirements and ethical concerns [19,20].

A key advantage of 3D printing technology is its design flexibility, which allows models to be customized through the selection of materials and printing parameters. These variables directly affect the mechanical properties of the models and their behavior during osteotomy [21–26]. Three-dimensional-printed models need to be highly realistic to replace cadaver models in surgical training. The models must provide realistic drilling properties such as hardness, vibration, and tactile feedback [9,27]. Although 3D printing is widely accessible, there is no standardized method to produce cost-effective and realistic bone models. University hospitals and training institutions have therefore developed their own approaches, testing various materials and printing parameters to achieve optimal results [25]. This lack of standardization in the field of 3D-printed medical models limits the consistency and quality of training, and the broader adoption in medical education.

Recent studies have adopted various approaches to validate 3D-printed bone models. Material comparisons have often focused on specific anatomical applications, particularly temporal bone simulation [28,29]. More recent studies have compared the haptic feedback of different printing technologies and materials during simulated implant surgery [30], evaluated polyethylene terephthalate glycol (PETG), Simubone™, and photopolymer resin for temporal bone simulation [31], and examined dimensional accuracy and surgeon-perceived performance across different additive manufacturing technologies [32]. Requena-Pérez et al. [33] developed fused filament fabrication (FFF)-printed femoral models with differentiated cortical and cancellous structures and assessed them in blinded surgical trials. Meanwhile, Weinschenk et al. [34] investigated the effects of printing parameters on the flexural behavior of polylactic acid (PLA) femoral models. Despite these advances, evidence remains limited on whether mechanical similarity to a biological reference corresponds to perceived haptic realism across multiple fused deposition modeling (FDM) materials and different osteotomy instruments.

This study addresses this gap by taking an integrated, application-oriented approach combining printing-parameter selection based on mechanical testing with user evaluation. First, the effects of infill density, infill pattern and the number of outer layers on maximum bending force were systematically investigated in four FDM materials using three-point bending tests with porcine ribs as a biological reference. A standardized model architecture was evaluated by students and doctors using three osteotomy instruments with different cutting mechanisms. In addition to perceived haptic realism, the osteotomy duration

and material-specific surface artifacts were assessed. By linking mechanical performance with user perception, this study aims to identify the strengths and limitations of PLA, PETG, acrylonitrile styrene acrylate (ASA) and polycarbonate (PC), and to provide printing recommendations for cost-effective osteotomy training models.

## 2. Materials and Methods

The experimental process consisted of three phases. First, a computed tomography (CT)-based porcine rib model was developed and manufactured using four FDM materials. Second, three-point bending tests were performed to investigate the effects of printing parameters and select a standardized model configuration, using the porcine ribs as a biological reference. Third, students and doctors performed osteotomies on the porcine reference model and the four printed models using three different instruments. The printed models were then evaluated based on user ratings, osteotomy duration, and material-specific surface artifacts.

### *2.1. Study Design*

The primary endpoint was the difference in the numerical rating scale (NRS) in haptic properties during osteotomy between the various 3D-printed materials and a porcine rib. Secondary endpoints comprised the difference in NRS scores between the two cohorts regarding the comparability of osteotomy behavior of the 3D-printed models with the natural porcine rib, a blinded evaluation of the models regarding melting, stringing, and fraying on a Likert scale by M.B. and L.G., a comparison of osteotomy time between the models and the porcine rib as well as an assessment of the maximum bending force of the 3D-printed models compared with the porcine rib using a three-point bending test.

The study protocol was registered with the German Clinical Trials Register (DRKS00034343, registration date 30 October 2024). The trial was successfully conducted between 7 December 2024 and 19 January 2025 in the Department of Oral and Maxillofacial Surgery of the University Hospital Aachen, Germany.

### *2.2. Model Development*

Four commercially available FDM filaments produced by Polymaker (Shanghai, China) were investigated: polylactic acid (PLA), acrylonitrile styrene acrylate (ASA), polyethylene terephthalate glycol (PETG), and polycarbonate (PC). All materials had the color white. The materials were selected based on their commercial availability, compatibility with desktop FDM printing, and differing thermal characteristics. PLA, PETG, and PC have previously been investigated for the fabrication of anatomical or surgical training models [29,31,34]. ASA was selected as an alternative to acrylonitrile butadiene styrene (ABS) because of concerns regarding the comparatively high volatile organic compound emissions associated with ABS printing [35]. Together, the four materials provided a range of glass-transition temperatures and material behaviors for evaluation during osteotomy.

Porcine ribs were selected as the biological reference because they have structural and cortical characteristics relevant to the human mandible [36]. Fourteen porcine ribs were tested to establish the mechanical reference value. The rib segment selected as the anatomical template had a curved, asymmetric geometry and measured 108 mm in length, with a maximum height of 21 mm and a maximum width of 11 mm. Maximum force (Fmax, N) was the only mechanical parameter extracted from the three-point bending tests and was used to compare the printed models with the porcine reference. The availability of porcine ribs and the comparatively limited ethical constraints enabled repeated mechanical testing.

The template of the porcine rib was taken from a computed tomography (CT) dataset, segmented manually based on the bone threshold in 3D slicer (version 5.2.1; The Slicer

Community, USA) and exported as a Standard Tessellation Language (STL) file. The model was subsequently smoothed and trimmed in Blender (version 3.4.1). In addition, a separate external fixation device was designed to secure the rib model during osteotomy (Figure 1 and Supplementary Figure S1).



**Figure 1.** Experimental setup showing the fixation of a 3D-printed model on a laboratory table during osteotomy procedures.

Table 1 summarizes the relevant material properties and material-specific printing temperatures. While the four filaments had similar densities, their glass-transition temperatures increased from PLA to PETG, ASA, and PC. Consequently, higher nozzle and heat bed temperatures were used for ASA and PC than for PLA and PETG.

**Table 1.** Material properties and printing parameters of the investigated FDM filaments.

| Material | Commercial Product | Manufacturer Product Code | Density (g/cm$^3$) | Glass-Transition Temperature (°C) | Nozzle Temperature Used (°C) | Heat-Bed Temperature Used (°C) |
|---|---|---|---|---|---|---|
| PLA | PolyLite™ PLA, white | PA02002 | 1.17 | 61 | 215 | 60 |
| PETG | PolyLite™ PETG, white | PB01052 | 1.25 | 81 | 230 | 85 |
| ASA | PolyLite™ ASA, white | PF01002 | 1.13 | 97.8 | 260 | 100 |
| PC | PolyMax™ PC, white | 70490 | 1.19 | 113 | 270 | 100 |

Density and glass-transition temperature values were obtained from the manufacturers' technical data sheets and were not measured independently in this study.

All models were printed with a Prusa MINI+ (Prusa Research, Prague, Czech Republic). The extrusion nozzle has a diameter of 0.4 mm. The slicer used is the free PrusaSlicer (version 2.7.0 and subsequent updates; Prusa Research, Prague, Czech Republic). Three printing parameters were varied: the number of outer layers (2–4 layers; nominal line width approximately 0.45 mm), the infill density (5–100%) and the infill pattern (gyroid, 3D honeycomb, rectilinear). Printing was performed without an enclosed build chamber (Table 2). Printability was not systematically assessed or recorded as a study endpoint.

**Table 2.** Equipment and printing parameters used for the printing trials.

| Parameter | Setting |
|---|---|
| 3D printer | Original Prusa MINI+ (Prusa Research, Prague, Czech Republic) |
| Slicing software | PrusaSlicer (version 2.7.0 and subsequent updates; Prusa Research, Prague, Czech Republic) |

**Table 2.** *Cont.*

| Parameter | Setting |
|---|---|
| Filament diameter | 1.75 mm |
| Nozzle diameter | 0.4 mm |
| Layer height | 0.2 mm |
| Outer layers | 2–4 |
| Infill density | 5–100% |
| Infill patterns | Gyroid, 3D honeycomb, and rectilinear |
| Enclosure | Not used |

### 2.3. Three-Point Bending Tests and Parameter Selection

Preliminary three-point bending tests were conducted to select a standardized model configuration for the subsequent participant evaluation. The tests were performed using a Zwick universal testing machine (ZwickRoell GmbH & Co. KG, Ulm, Germany), following a test protocol based on DIN EN ISO 178 [37]. Porcine ribs and 3D-printed models were examined using the same testing procedure. Each specimen was positioned on two supports with a span of 60 mm, and the load was applied centrally between the supports. After application of a preload of 5 N, the specimens were loaded at a constant displacement rate of 5 mm/min. Force and displacement were recorded continuously to generate force–displacement curves. The maximum force (Fmax, N) was extracted from each curve and used as the mechanical comparison parameter. Fourteen porcine ribs were tested to establish the biological reference value. A total of 96 models were manufactured from the four materials using different printing-parameter combinations and examined using the same testing procedure. The printed models were subsequently tested under identical conditions, and their maximum forces were compared descriptively with the mean maximum force of the porcine ribs.

First, infill density and the number of outer layers were varied systematically. In a second series, models differing only in infill pattern were tested to assess this parameter while keeping the remaining printing parameters constant. Linear regression was used to estimate material-specific parameter combinations approaching the mean maximum bending force of the porcine ribs. The selected configurations were subsequently examined in an additional three-point bending test. The number of outer layers was set to two, corresponding to a nominal shell thickness of approximately 0.90 mm to approximate the anatomical conditions of porcine ribs [38]. In addition, a specialist in oral and maxillofacial surgery (B.P.) and a dentist (L.G.) from Aachen University Hospital performed preliminary osteotomies on models printed with 25% infill and each of the three investigated infill patterns. Based on the preliminary mechanical testing and practical evaluation, a standardized configuration of 25% gyroid infill and two outer layers was selected for the subsequent participant evaluation.

### 2.4. Sample Size Calculation

For the sample size calculation, a minimum effect of 0.5 points on the NRS was assumed between the materials. It was performed in R (Version R4.3.3, www.r-project.org). With a significance level of $\alpha = 0.05$ and a test power of 80%, a common standard deviation of 2.06 was assumed for the four materials ASA, PC, PETG and PLA based on the literature [28]. This results in an effect size of $f = 0.5/2.06 = 0.243$. The required number of cases is therefore 28 participants for a repeated-measures analysis of variance (ANOVA) with a within-between factor interaction. To compensate for non-evaluable data sets and possible study dropouts, two additional participants per cohort were planned.

### 2.5. Participants and Osteotomy Evaluation

A total of 32 participants took part in this cohort study, including 16 dental or medical students and 16 doctors with different levels of osteotomy experience. The study was conducted over four weekends. After providing informed consent, participants completed a questionnaire collecting information on age, sex, and previous experience with osteotomies and surgical equipment (Table 3). A standardized within-participant design was used: every participant evaluated all four materials using each of the three instruments and therefore served as their own control. The order of models for osteotomy was randomized for each participant. Slips of paper containing all possible permutations were prepared in two bowls; one was randomly drawn at the beginning for each participant and not returned. Material identity was concealed throughout testing. All models were printed in identical white color and labeled exclusively with numerical identifiers, preventing participants from identifying the respective material.

**Table 3.** Characteristics of the study participants ($n$ = 32).

| | | **Doctors ($n$ = 16)** | **Students ($n$ = 16)** | **Total ($n$ = 32)** |
|---|---|---|---|---|
| Age | mean (SD) | 30 (4.8) | 22.9 (1.9) | 26.5 (5.1) |
| Gender | female<br>male | 4 (25%)<br>12 (75%) | 10 (62.5%)<br>6 (37.5%) | 14 (43.8%)<br>18 (56.2%) |
| Study Program | Medicine<br>Dentistry | -<br>- | 2 (12.5%)<br>14 (87.5%) | -<br>- |
| Clinical Semester | mean (SD) | - | 8.1 (3.7) | - |
| Discipline | OMFS<br>Prostodontics<br>Restorative dentistry | 12 (75%)<br>2 (12.5%)<br>2 (12.5%) | -<br>-<br>- | -<br>-<br>- |
| Work Experience | Years mean (SD) | 4 (3.5) | - | - |
| Osteotomies made | mean (SD) | 163.3 (297.3) | 15.9 (62.4) | 89.6 |
| Preferred instrument, $n$ (% of selections) | Conventional Bur<br>Ultrasonic Device<br>Reciprocating Saw | 7 (36.8%)<br>7 (36.8%)<br>5 (26.3%) | 4 (80%)<br>1 (20%)<br>0 | |

Data are presented as mean (SD) or $n$ (%). SD, standard deviation; OMFS, oral and maxillofacial surgery; -, not applicable. Multiple responses were permitted for preferred instrument; percentages refer to the total number of selections within each cohort.

Participants were provided with lab coats, safety goggles and nitrile gloves. The porcine rib and the four printed models were secured to a laboratory table using five fixation devices. Three osteotomy systems were used: a conventional Lindemann bur (H254E, Komet/Gebr. Brasseler GmbH & Co. KG, Lemgo, Germany) and a reciprocating Saw GP543R (B.Braun SE, Melsungen, Germany) were used with the ELAN 4 System (Aesculap AG, Tuttlingen, Germany) and an ultrasonic attachment OT7S-4 was used with the PIEZOSURGERY® System (Mectron Medical Technology, Carasco, Italy). Watercooling was set to 100%. To ensure comparable testing conditions, model geometry, fixation, predefined osteotomy lines, instrument settings, water cooling, instructions, and questionnaires were standardized for all participants. The osteotomy was first performed on the porcine rib with each of the three instruments. Lines for the osteotomies were marked on the rib and on the models. Following this, the participants proceeded to osteotomize the four models in the same manner as they had done with the porcine rib before.

After each osteotomy procedure, participants evaluated three items using a numerical rating scale (NRS) ranging from 0 to 10: haptic feedback compared with the porcine

reference, self-assessed learning effect, and teaching usefulness. Higher scores indicated a more favorable assessment. The duration of each osteotomy was recorded. After completing all osteotomies, participants answered a structured questionnaire with six four-point Likert items (1 = strongly disagree, 4 = strongly agree), selected their preferred material, and provided open-ended feedback. Participants also rated the tactile similarity of the porcine rib to human bone for each instrument. The selection of questions was informed by prior studies [39,40] and the 3D Printing Data Dictionary (3DPDD) published by the Radiological Society of North America (RSNA) and the American College of Radiology (ACR) in 2024 [41].

Following osteotomy, melting, fraying, and stringing were rated on a three-point scale (0 = none, 1 = moderate, 2 = strong) by two investigators (M.B. and L.G.) who were blinded to material identity. Disagreements were resolved by consensus.

Following the conclusion of the study, all data were anonymized in accordance with the study protocol.

### 2.6. Statistical Analysis

Statistical analyses were performed using R (version 4.3.3). A $p$-value of $<0.05$ was considered statistically significant. Normality of residuals was assessed visually and was considered acceptable for all models.

The primary endpoint was analyzed using a linear mixed-effects model with material and cohort as fixed effects and participant as a random effect. Secondary endpoints, including cohort comparisons and osteotomy duration, were analyzed using linear mixed-effects models (LMM). Melting, fraying and stringing were evaluated using a 3-point Likert scale by two blinded investigators (M.B., L.G.) who reached a consensus rating. As only one rating per model was available and the data were ordinal, comparisons between materials were performed using the Kruskal–Wallis test, followed by Dunn's post hoc test with Bonferroni correction.

Participant characteristics and questionnaire responses were summarized using means and standard deviations for numerical variables, as well as frequencies and percentages for categorical variables. The six four-point Likert items, preferred material selections, and instrument-specific ratings of the porcine reference were analyzed descriptively. Open-ended responses were summarized narratively.

## 3. Results

The doctors group consisted of 4 females and 12 males with a mean age of 30.0 years (range: 24.0–38.0 years). The student group consisted of 10 females and 6 males with a mean age of 22.9 years (range: 19.0–26.0 years). Previous experience with osteotomies or surgical training models was self-reported. Doctors reported a mean of 163.3 osteotomies performed (range: 0–1000), while students reported a mean of 15.9 (range: 0–250). One student reported performing 250 osteotomies, representing a clear outlier. Only two students reported any previous experience with osteotomies, and excluding the outlier, the average is significantly lower. The evaluation comprised a total of 128 models.

### 3.1. Haptic Feedback

Ratings of NRS Question 1 (haptic feedback) were defined as the primary endpoint and varied only minimally across the four models. PC received the highest scores ($\bar{x}$ = 6.7, SD = 1.8), followed by ASA ($\bar{x}$ = 6.4, SD = 1.9), PETG ($\bar{x}$ = 6.0, SD = 2.2), and PLA ($\bar{x}$ = 5.9, SD = 2.2). In the mixed-effects analysis, only PC was rated significantly higher than PLA (LMM, $p$ = 0.029).

Ratings of NRS Question 2 (self-assessed learning effect) also showed only modest differences between materials. ASA achieved the highest ratings ($\bar{x}$ = 6.9, SD = 2.7), followed by PC ($\bar{x}$ = 6.7, SD = 2.7), PETG ($\bar{x}$ = 6.5, SD = 2.8), and PLA ($\bar{x}$ = 6.3, SD = 2.7). The mixed model indicated a significant advantage for ASA over PLA (LMM, $p$ = 0.019).

Ratings of NRS Question 3 (teaching usefulness) showed a comparable distribution. ASA again received the highest ratings ($\bar{x}$ = 7.3, SD = 2.0), followed by PC ($\bar{x}$ = 7.2, SD = 2.0), PETG ($\bar{x}$ = 6.8, SD = 2.2), and PLA ($\bar{x}$ = 6.8, SD = 2.3). ASA received a significantly higher score than PLA (LMM, $p$ = 0.031) (Figure 2).

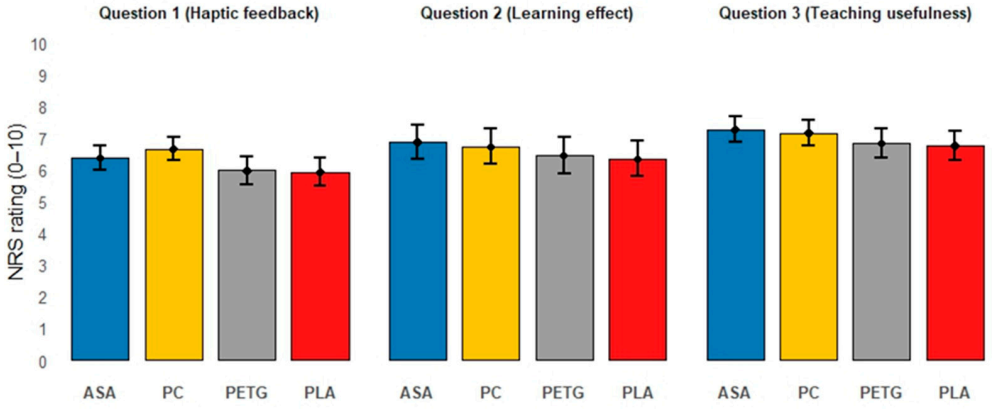



**Figure 2.** Mean NRS ratings (0–10) for Question 1 (haptic feedback), Question 2 (self-assessed learning effect), and Question 3 (teaching usefulness), stratified by material ($n$ = 32). Error bars indicate 95% confidence intervals.

### *3.2. Three-Point Bending Test and Parameter Selection*

The force–displacement curves of the 14 porcine ribs used to establish the biological reference are shown in Figure 3. Preliminary three-point bending tests showed that maximum bending force varied with infill density and the number of outer layers (Figure 4). Infill density produced the most pronounced differences in maximum bending force, whereas only minor differences were observed among the investigated infill patterns (Figure 5). Linear regression was used to estimate material-specific parameter combinations approaching the mean maximum bending force of the porcine ribs (Figure 6).

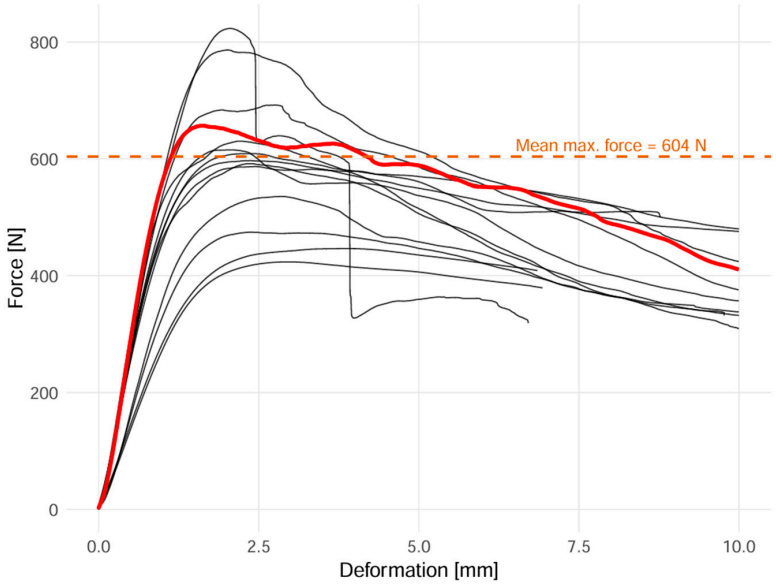



**Figure 3.** Force–displacement curves from three-point bending tests of porcine ribs ($n$ = 14). The selected reference rib is the red line.

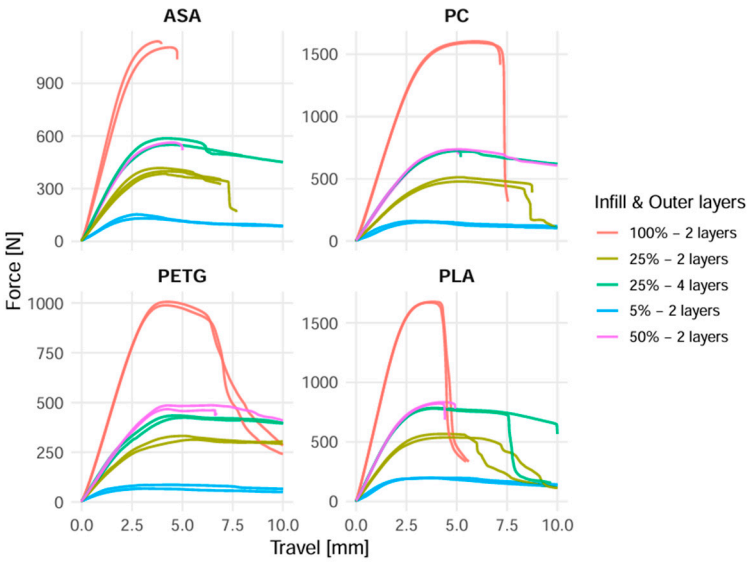



**Figure 4.** Influence of infill density and number of outer layers on maximum force (Fmax) obtained from three-point bending tests of 3D-printed rib models.

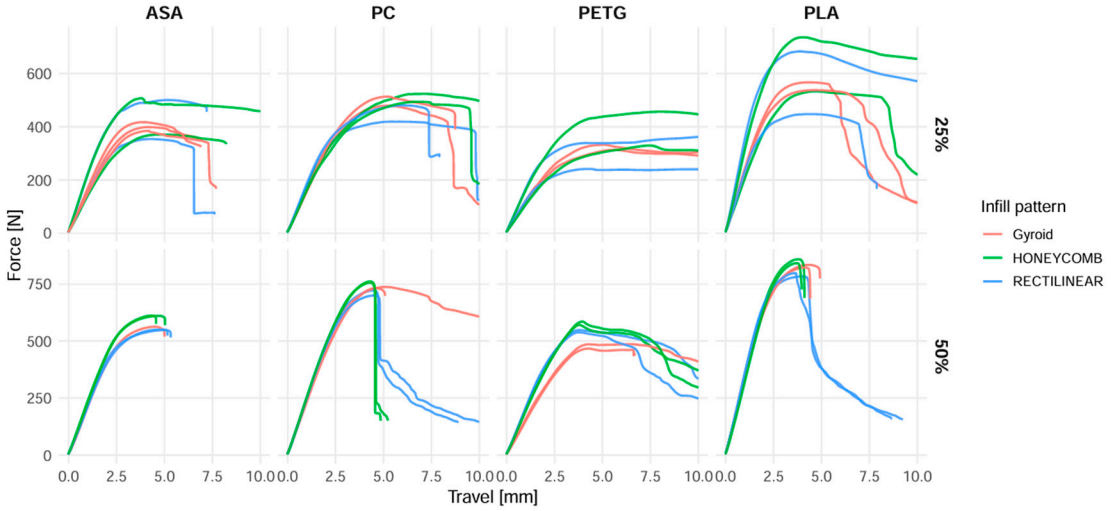



**Figure 5.** Comparison of maximum force (Fmax) obtained in three-point bending tests of 3D-printed rib models with different infill patterns (gyroid, 3D honeycomb, rectilinear).

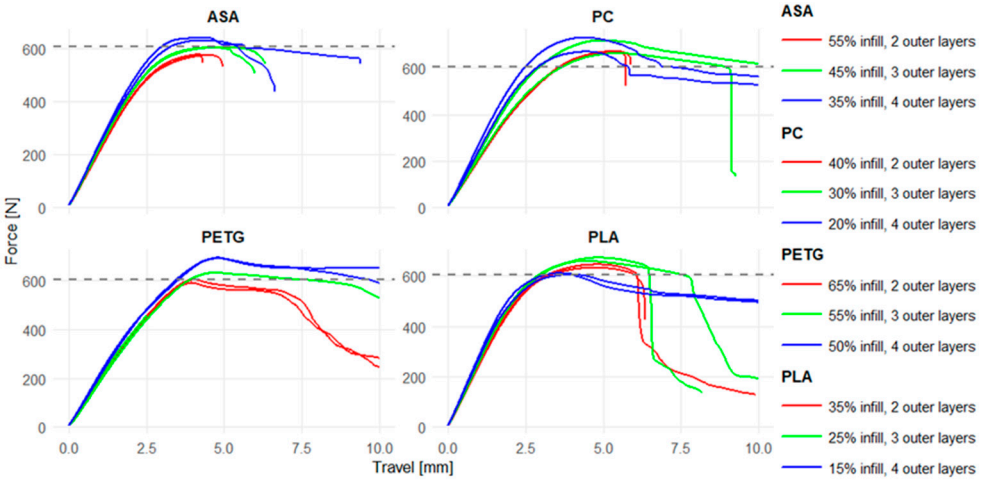



**Figure 6.** Force–displacement curves obtained from three-point bending tests of rib models after parameter optimization. The dotted line indicates the reference value derived from the porcine rib.

During the preliminary practical evaluation, both evaluators (B.P. and L.G.) preferred the gyroid infill pattern. They reported that its continuous three-dimensional internal structure reduced sudden penetration of the osteotomy instruments into the model. Based on the combined mechanical and practical findings, a standardized configuration of 25% gyroid infill and two outer layers was selected for the subsequent material comparison and participant evaluation.

The force–displacement curves of the models manufactured using the final configuration of 25% gyroid infill and two outer layers ($n$ = 2 per material) are shown in Figure 7. The 14 porcine ribs reached a mean maximum bending force of 604.9 ± 115.0 N and served as the biological reference. Among the printed materials, PLA exhibited the highest mean maximum bending force (552.1 ± 20.7 N), followed by PC (496.0 ± 24.5 N), ASA (408.0 ± 13.2 N), and PETG (322.9 ± 13.4 N). Thus, PLA showed the smallest numerical difference from the biological reference, followed by PC.

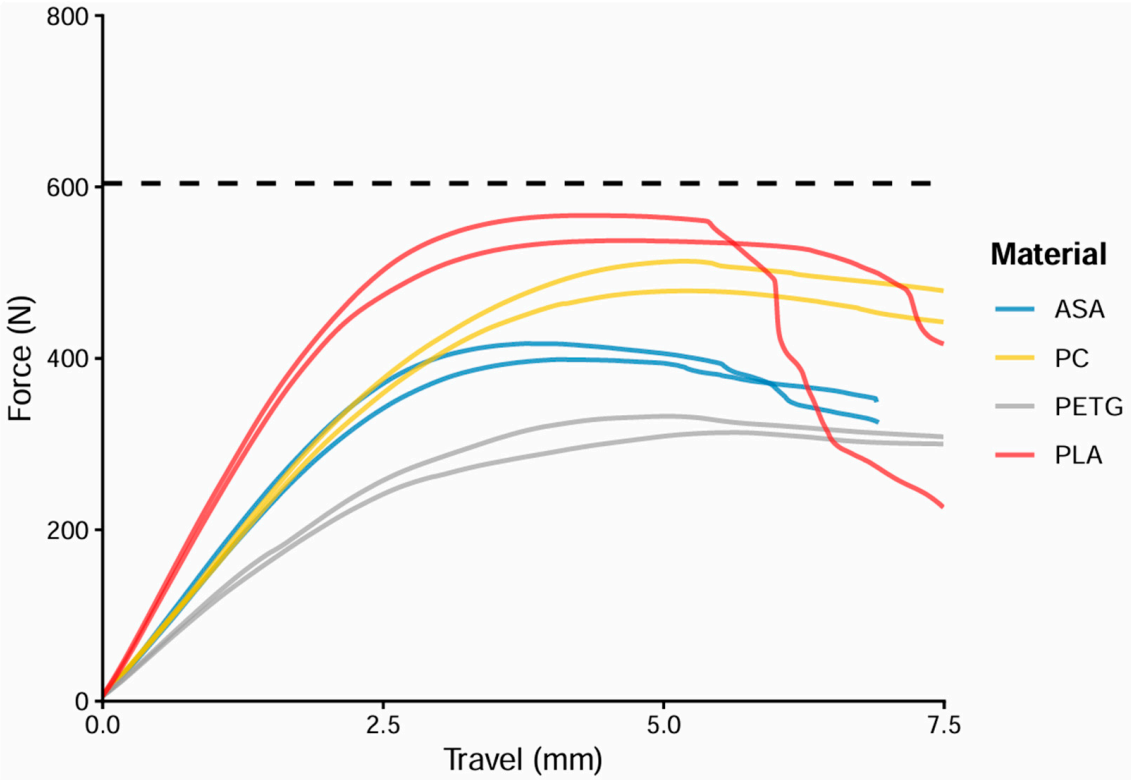



**Figure 7.** Force–displacement curves obtained from three-point bending tests of models fabricated from ASA, PC, PETG, and PLA using 25% gyroid infill and two outer layers. Each curve represents an individual measurement. The dashed horizontal line indicates the mean maximum bending force of the porcine ribs (604.9 N).

### *3.3. Osteotomy Duration*

Osteotomy duration was evaluated as a secondary endpoint. It varied across instruments and target materials. PLA most closely approximated porcine rib osteotomy time for both the Lindemann bur (rib: $\bar{x}$ = 24.8 s; PLA: $\bar{x}$ = 20.5 s; difference (Δ) = 4.3 s) and the Piezo device (rib: $\bar{x}$ = 37.4 s; PLA: $\bar{x}$ = 29.2 s; Δ = 8.2 s). In contrast, osteotomy times obtained with the reciprocating saw were similar across all materials, with PETG showing the smallest deviation from the rib (rib: $\bar{x}$ = 4.7 s; PETG: $\bar{x}$ = 4.8 s; Δ = 0.1 s) (Figure 8).

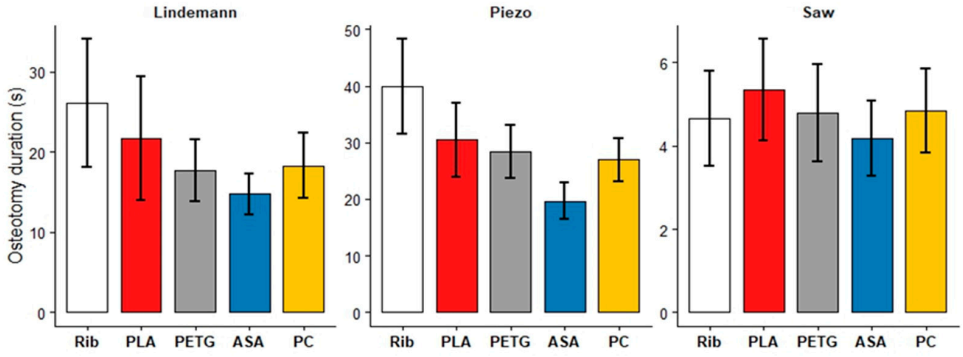



**Figure 8.** Mean osteotomy duration (seconds) for the porcine rib and 3D-printed models, stratified by instrument and material ($n$ = 32 per condition). Error bars indicate 95% confidence intervals.

### *3.4. Surface Artifacts After Osteotomy*

Surface artifacts (melting, fraying, and stringing) were evaluated as a secondary endpoint. Significant differences were observed between the materials (Kruskal–Wallis test, $p < 0.001$ for all). PETG ($\bar{x}$ = 1.4, SD = 0.5) and PLA ($\bar{x}$ = 1.3, SD = 0.6) showed the highest scores for melting while ASA ($\bar{x}$ = 0.8, SD = 0.7) and PC ($\bar{x}$ = 0.8, SD = 0.4) received lower ratings. In terms of fraying, again PETG ($\bar{x}$ = 1.1, SD = 0.2) and PLA ($\bar{x}$ = 0.9, SD = 0.6) achieved higher scores than ASA ($\bar{x}$ = 0.8, SD = 0.5) and PC ($\bar{x}$ = 0.3, SD = 0.5). Stringing was more present for ASA ($\bar{x}$ = 1.3, SD = 0.6) and PC ($\bar{x}$ = 0.9, SD = 0.7) than for PETG ($\bar{x}$ = 0.2, SD = 0.4) and PLA ($\bar{x}$ = 0.1, SD = 0.3). Post hoc analysis using Dunn's test with Bonferroni correction confirmed that PETG exhibited significantly higher melting compared with ASA and PC (both $p < 0.001$), and PLA also showed higher melting than ASA ($p$ = 0.011) and PC ($p$ = 0.028). For fraying, PETG and PLA scored significantly higher than PC (both $p < 0.001$). ASA and PC showed significantly more stringing than PETG and PLA (all $p < 0.001$) (Figure 9).

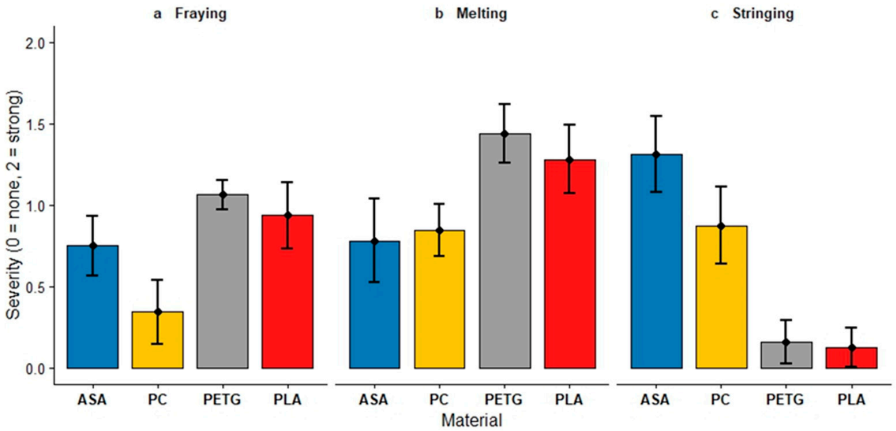



**Figure 9.** Blinded evaluation of surface artifacts after osteotomy, rated on a three-point scale (0 = none, 2 = strong) for each material. Bars represent mean severity scores, and error bars indicate 95% confidence intervals.

### *3.5. Instrument Rating*

In addition to the predefined endpoints, further analyses were conducted. Across all three evaluation criteria, the reciprocating saw achieved the highest ratings (haptic feedback: $\bar{x}$ = 7.1, SD = 1.7; self-assessed learning effect: $\bar{x}$ = 7.2, SD = 2.6; teaching usefulness: $\bar{x}$ = 7.5, SD = 2.0). The Lindemann bur received intermediate scores (6.1 ± 1.9; 6.3 ± 3.0; 7.1 ± 2.2), while the Piezo instrument consistently ranked lowest (5.5 ± 2.2; 6.3 ± 2.5; 6.5 ± 2.2). These findings indicate that participants considered the reciprocating saw most suitable for training, whereas the Piezo device was perceived as less appropriate.

### *3.6. Cohort Differences*

Cohort differences between students and doctors were analyzed as a secondary endpoint. Across all three NRS questions, students tended to give slightly higher ratings than doctors. However, no statistically significant differences between cohorts were observed. For Question 1 (haptic feedback), cohort had no significant effect on ratings ($p = 0.575$). Similarly, no cohort-related differences were found for Questions 2 and 3 (LMM, self-assessed learning effect and teaching usefulness; $p = 0.182$ and $p = 0.597$). Despite differing levels of clinical experience, students and doctors rated the models quite similarly. Both groups rated PC and ASA best for haptic feedback (students: $\bar{x} = 6.75$ and 6.54; doctors: $\bar{x} = 6.56$ and 6.19), while PETG and PLA got lower scores (Figure 10).

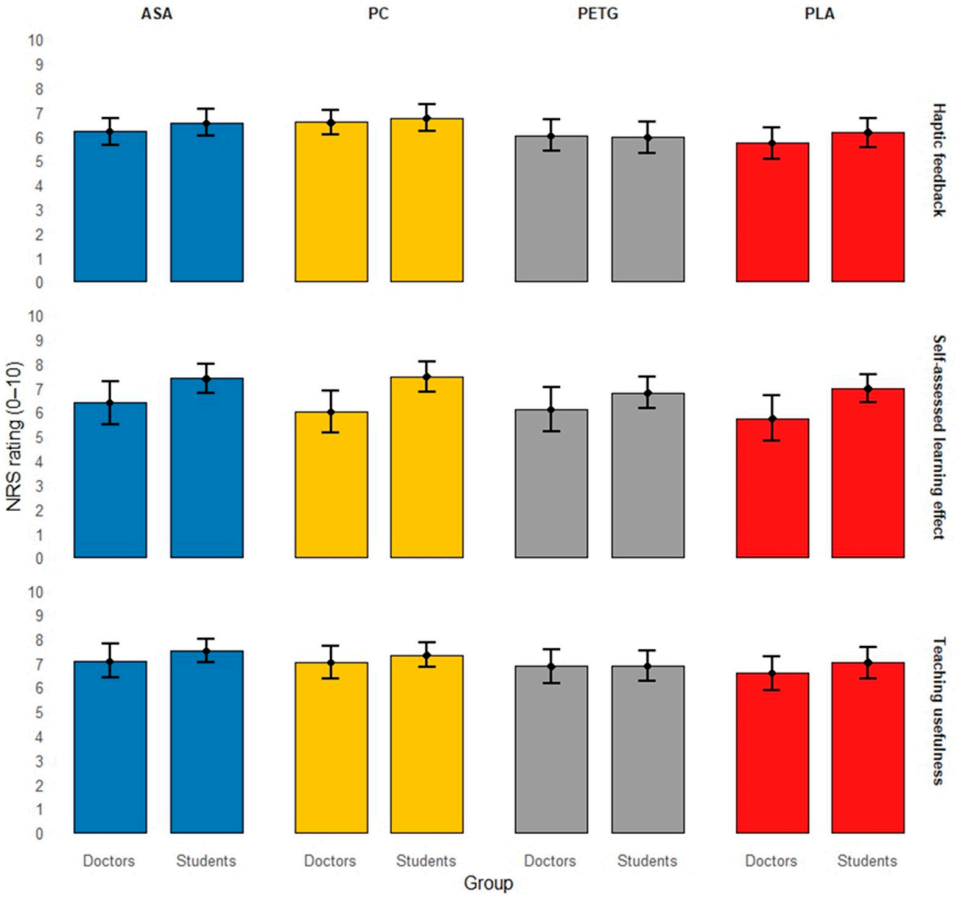



**Figure 10.** Mean NRS ratings (0–10) for Question 1 (haptic feedback), Question 2 (self-assessed learning effect), and Question 3 (teaching usefulness), stratified by material and cohort (students vs. doctors, $n = 32$). Error bars indicate 95% confidence intervals.

### *3.7. Likert Questions and Open Questions*

The final evaluation of the 3D-printed models through six Likert questions revealed a high level of acceptance among both students and doctors, especially for their low cost and ease of use (Table 4).

**Table 4.** Likert questions (1 = fully disagree, 4 = fully agree).

| Mean (SD) | Doctors | Students | Total |
|---|---|---|---|
| The 3D-printed models were easy to use. | 3.81 (0.4) | 3.88 (0.3) | 3.84 (0.4) |
| After performing osteotomies on the 3D-printed models, I feel more confident in handling the instruments used. | 3.25 (0.9) | 3.44 (0.8) | 3.34 (0.9) |

**Table 4.** *Cont.*

| Mean (SD) | Doctors | Students | Total |
|---|---|---|---|
| The widespread use of 3D-printed bone models improves training. | 3.44 (0.9) | 3.75 (0.5) | 3.59 (0.7) |
| I find the surface texture of the models similar to that of a human bone. | 3 (0.5) | 3.25 (0.6) | 3.12 (0.6) |
| I consider these models a good substitute for cadaver bones in surgical training. | 3.44 (0.8) | 3.5 (0.6) | 3.47 (0.7) |
| I consider the material cost of approximately €1 for a complete mandible model to be reasonable. | 3.94 (0.3) | 4 (0) | 3.97 (0.2) |

Participants were asked to indicate their preferred material. Among doctors, PC was chosen most frequently ($n$ = 6), followed by ASA ($n$ = 4), PLA ($n$ = 3), and PETG ($n$ = 3). Most students preferred ASA ($n$ = 10), with fewer selecting PC ($n$ = 4) or PETG ($n$ = 2). In one case, a student evaluated two materials; for the purpose of analysis, only one material (ASA) was included, without a defined selection order (Figure 11).

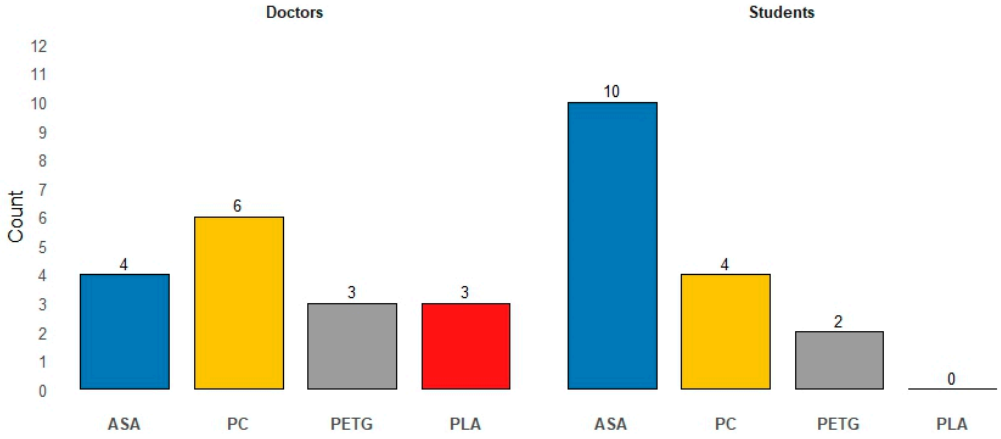



**Figure 11.** Distribution of preferred materials among doctors and students ($n$ = 32). Bars represent the number of selections for each material within each group.

In the open-ended responses, participants frequently mentioned that all materials were very similar. Additionally, the cortex and bone marrow could be easily distinguished during osteotomies. The models were perceived as an ideal opportunity to practice using the instruments. Some expressed concern about the short osteotomy lines marked on the models.

Participants were asked to assess the suitability of a porcine rib as a comparative model for human bone by rating the tactile similarity during osteotomy procedures. The reciprocating saw received the highest rating ($\bar{x}$ = 8.72, SD = 1.13), followed by the ultrasonic device ($\bar{x}$ = 7.20, SD = 1.77) and the Lindemann bur ($\bar{x}$ = 6.90, SD = 2.14).

## 4. Discussion

This study evaluated four commonly used FDM materials (ASA, PC, PETG and PLA) for producing 3D-printed bone models used in osteotomy training. While no material was statistically superior for the primary endpoint of haptic feedback, ASA and PC received the highest subjective ratings, indicating a closer approximation of bone-like tactile behavior during osteotomy. This aligns with previous studies showing that material performance depends on the specific surgical application, and no material is universally superior. Haffner et al. identified PETG as favorable for temporal bone simulation, while McMillan et al. have identified several materials suitable for surgical drilling training, including PC used with an FDM printer [28,29].

Consistent with the subjective evaluation results, participants expressed a preference for PC and ASA. Students more frequently favored ASA, likely due to its lower cutting resistance. Experienced doctors tended to prefer PC because of its greater stiffness and closer tactile resemblance to bone. These results suggest that the suitability of a material may depend on the learner's level of experience, and they highlight the potential of customizable models to support differentiated training approaches.

The three-point bending tests demonstrated that PLA most closely approximated the mean maximum bending force of the porcine ribs, followed by PC. However, similarity in maximum bending force did not directly correspond to perceived haptic realism, as PC and ASA received higher haptic ratings than PLA. This discrepancy suggests that maximum bending force alone is insufficient to determine the suitability of a 3D-printed model for osteotomy training. Other material-dependent characteristics, including deformation and fracture behavior, thermal response, and interaction with the cutting instrument, may also influence tactile perception during osteotomy. Therefore, biomechanical testing and user-based evaluation should be regarded as complementary approaches when selecting materials for surgical training models.

Differences related to the instrument were more pronounced than effects related to the material. The reciprocating saw received the highest ratings in all categories, likely because its cutting mechanism primarily relies on mechanical material removal, making it less sensitive to variations in thermoplastic properties. In contrast, the piezoelectric device performed less favorably because high-frequency oscillations generated heat, which led to melting rather than effective cutting. This differs from natural bone, where mineralized tissue enables microfracturing instead of thermal deformation [42]. The Lindemann bur showed intermediate ratings, indicating that, although cortical resistance was not fully replicated, the models permitted the realistic practice of drilling techniques.

The material-specific surface artifacts may be explained by differences in thermal and deformation behavior during osteotomy. PLA and PETG have lower glass-transition temperatures than ASA and PC and may therefore soften more readily when exposed to frictional heat generated by the cutting instruments. Local softening can promote material smearing, melting, and irregular frayed edges. In contrast, the higher thermal resistance of ASA and PC may explain the lower melting scores observed for these materials. However, once locally softened, their viscoelastic and ductile behavior may allow the polymer to be drawn into strands during instrument movement or withdrawal, resulting in more pronounced stringing. These mechanisms were not measured directly in the present study and should therefore be interpreted as plausible material-dependent explanations for the observed artifact patterns.

Students generally rated the models slightly higher than doctors did, especially regarding the perceived benefit of learning (students: haptic feedback: $\bar{x} = 6.3$, SD = 2.0; learning effect: $\bar{x} = 7.2$, SD = 2.1; teaching usefulness: $\bar{x} = 7.2$, SD = 1.9; doctors: haptic feedback: $\bar{x} = 6.1$, SD = 2.1; learning effect: $\bar{x} = 6.1$, SD = 3.1; teaching usefulness: $\bar{x} = 6.9$, SD = 2.3; all $p > 0.182$). This difference likely reflects varying levels of clinical experience, as less experienced participants may benefit more from the structured, low-risk nature of simulated training environments. Educational theory emphasizes the importance of such settings for early skill acquisition because they allow for repetition and progressive familiarization without risking patient safety [19,43]. Despite these tendencies, however, the overall rating patterns were similar between the two groups, indicating that both students and doctors assessed the suitability of the material in a largely consistent manner.

The survey results showed that the models were highly accepted, especially for their cost-effectiveness, realism, and educational usefulness. These results align with previous

studies indicating that 3D-printed models can rival or surpass synthetic or cadaveric models in terms of anatomical accuracy, operative simulation, and accessibility [12,27,44–49].

From an economic perspective, FDM-based model production offers substantial cost advantages. Based on the current purchase price of approximately $590 (€509) for the desktop printer used in this study (Original Prusa MINI+, Prusa Research, Prague, Czech Republic), the initial investment is offset after printing a relatively small number of models. Using PolyMax™ PC filament (Polymaker, Shanghai, China) at approximately $52 (€45) per 750 g spool, the material cost is about $0.07 per gram. Thus, a rib model with a filament consumption of 10 g costs about $0.70, whereas a mandibular model requiring 30 g costs about $2.10 (as of April 2026).

In comparison, commercially available models are substantially more expensive. For example, an edentulous Sawbones mandible (Pacific Research Laboratories, Vashon, WA, USA) costs approximately $15, meaning the initial printer cost would be recovered after 39 mandibular models. A more functionally comparable alternative is the polyurethane fracture simulation model from SYNBONE AG (Zizers, Switzerland), priced at approximately $40 (32 Swiss francs, CHF). This results in a break-even point after 15 models. It is important to note that the lower-cost Sawbones model is primarily a static anatomical model, while the SYNBONE model enables fracture simulation and is therefore more comparable to the present training application. Overall, 3D-printed models are substantially cheaper, with a cost reduction of approximately one order of magnitude compared to commercially available alternatives. In addition to cost, production time remains practical: a rib model takes approximately 60 min to print, and a complete mandibular model takes approximately three hours. However, more advanced approaches, such as multi-material printing to simulate anatomical structures like nerves or bone marrow, may increase production time and require more expensive hardware, thereby reducing the cost advantage.

The perceived similarity of porcine ribs to human bones underpins their role as a useful reference standard in model development. Other animal models, such as bovine ribs, have also been described [50]. Rather than using porcine ribs as an anatomical substitute for the human mandible, they were used as a standardized biomechanical and haptic reference with cortical and cancellous bone structures. Their greater accessibility also allowed for repeated mechanical testing, which could not be done with the limited number of human mandibular specimens available. Although only three students had previous experience with osteotomies, many participated in the evaluation of the porcine ribs. Their ratings were retained to preserve data completeness.

Core printing parameters, including infill density, pattern, and outer shell thickness, were easily adjustable without advanced technical expertise. Furthermore, the selected printing parameters can be interpreted in the context of bone anatomy and manufacturing efficiency. Using two outer layers approximates the cortical bone structure of a porcine rib. This ensures realistic initial resistance during osteotomy, while reducing material consumption and printing time. Bending tests revealed that an infill density of 25% best replicates the flexural behavior of a porcine rib while enabling a haptic distinction between cortical strength and trabecular compliance. Higher infill densities resulted in greater stiffness, and lower densities reduced structural stability. The infill pattern did not significantly affect the bending properties. However, the continuous, three-dimensional gyroid structure enabled more homogeneous force distribution, improving haptic perception during osteotomy by preventing sudden drop-through of instruments. All selected parameters can be implemented using standard FDM settings without additional technical effort. This demonstrates that anatomically oriented and biomechanically validated models can be efficiently and reproducibly produced, facilitating their integration into surgical training. While print-

ing orientation may influence mechanical behavior, this aspect was not systematically evaluated and should be addressed in future studies.

Despite the promising results, several limitations should be acknowledged. The evaluation was based mostly on subjective ratings rather than objective performance metrics like accuracy or error rates. Additionally, the simplified rib model does not accurately represent the anatomical complexity of craniofacial structures. Initially planned biomechanical testing of human mandibles could not be performed due to limited specimen availability. While the sample size was sufficient for the primary endpoint, it may limit the study's generalizability, especially in subgroup analyses. Printability was neither systematically assessed nor recorded in the present study. Future studies should quantify material-specific printing behavior using predefined outcomes, such as the print failure rate, warping, dimensional accuracy, and the need for reprinting. Future research should incorporate objective performance measures and evaluate integrating standardized 3D-printed models into structured surgical curricula. Developing validated STL libraries with optimized printing parameters could improve reproducibility across institutions. Additionally, combining physical models with digital technologies, such as augmented reality, could improve simulation fidelity. While 3D-printed models cannot fully replicate human bone, they are a practical solution for repeated surgical training due to their low cost, adaptability, and ethical advantages. To support reproducibility, finalized STL files and slicer profiles are available upon request.

## 5. Conclusions

With a standardized configuration of 25% gyroid infill and two outer layers, PLA most closely approximated the mean maximum bending force of porcine ribs. However, PC achieved the highest haptic rating and was significantly higher than PLA. The reciprocating saw received the highest ratings across all evaluation criteria, indicating that the suitability of the printed models depended on the osteotomy instrument used. PETG and PLA exhibited more melting and fraying, while ASA and PC showed more stringing. These results demonstrate material-specific differences in cutting behavior. In conclusion, mechanical similarity does not directly correspond to perceived haptic realism. Therefore, both mechanical testing and user evaluation should be considered when selecting FDM materials for cost-effective osteotomy training models.

**Supplementary Materials:** The following supporting information can be downloaded at: https://www.mdpi.com/article/10.3390/app16178409/s1, Figure S1: Construction for attachment and rib model; Table S1: Mean (±SD) NRS ratings stratified by group, material, and instrument.

**Author Contributions:** Conceptualization, A.R., B.H.-P. and M.B.; methodology, M.B., Y.L. and B.H.-P.; software, M.B., L.G., and Y.L.; validation, M.B., L.G., Y.L., A.R., and B.H.-P.; formal analysis, M.B., Y.L. and B.H.-P.; investigation, M.B., L.G. and Y.L.; resources, F.H., R.R., M.M., A.R. and B.H.-P.; data curation, M.B. and Y.L.; writing—original draft preparation, M.B.; writing—review and editing, B.H.-P., M.B., A.R., Y.L., L.G., K.X., M.M., F.H., and R.R.; visualization, M.B., Y.L. and K.X.; supervision, B.H.-P., A.R.; project administration, B.H.-P.; funding acquisition, B.H.-P. All authors have read and agreed to the published version of the manuscript.

**Funding:** Behrus Hinrichs-Puladi was funded by the Medical Faculty of RWTH Aachen University as part of the Clinician Scientist Program.

**Institutional Review Board Statement:** The study was approved by the Institutional Review Board (or Ethics Committee) of University Hospital RWTH Aachen (protocol code EK 24-318; date of approval 09.09.2024, Prof. Dr. med. Ralf Hausmann, Prof. Dr. med. Günther Schmalzing).

**Informed Consent Statement:** Informed consent was obtained from all participants involved in the study.

**Data Availability Statement:** The data presented in this study are available on request from the corresponding author.

**Acknowledgments:** We would like to thank Jan Egger for his technical support with the software implementation and for his critical review of the manuscript and Axel Honné from the Scientific Workshop at Aachen University Hospital for creating the attachment construction. DeepL Translator (web-based version, continuously updated; DeepL SE, Cologne, Germany; accessed between November 2023 and August 2026) was used for translation and linguistic correction of the manuscript. During manuscript preparation, the authors used ChatGPT (web-based version, models available and continuously updated during the preparation period; OpenAI, San Francisco, CA, USA; accessed between November 2023 and August 2026) to assist in writing R code for statistical analysis and figure generation. The authors have reviewed and edited the output and take full responsibility for the content of this publication.

**Conflicts of Interest:** The authors declare no conflicts of interest.

## Abbreviations

The following abbreviations are used in this manuscript:

| Abbreviation | Definition |
|---|---|
| 3D | Three-Dimensional |
| 3DPDD | 3D Printing Data Dictionary |
| ABS | Acrylonitrile Butadiene Styrene |
| ACR | American College of Radiology |
| ANOVA | Analysis of Variance |
| ASA | Acrylonitrile Styrene Acrylate |
| CT | Computed Tomography |
| FDM | Fused Deposition Modeling |
| FFF | Fused Filament Fabrication |
| Fmax | Maximum Force |
| LMM | Linear Mixed-Effects Model |
| NRS | Numerical Rating Scale |
| OMFS | Oral and Maxillofacial Surgery |
| PC | Polycarbonate |
| PETG | Polyethylene Terephthalate Glycol |
| PLA | Polylactic Acid |
| RSNA | Radiological Society of North America |
| SD | Standard Deviation |
| STL | Standard Tessellation Language |

## References

1. Shahrezaei, A.; Sohani, M.; Taherkhani, S.; Zarghami, S.Y. The impact of surgical simulation and training technologies on general surgery education. *BMC Med. Educ.* **2024**, *24*, 1297. [CrossRef] [PubMed]
2. Hölzle, F.; Franz, E.-P.; Lehmbrock, J.; Weihe, S.; Teistra, C.; Deppe, H.; Wolff, K.-D. Thiel embalming technique: A valuable method for teaching oral surgery and implantology. *Clin. Implant Dent. Relat. Res.* **2012**, *14*, 121–126. [CrossRef] [PubMed]
3. Chen, X.; Hu, J. A review of haptic simulator for oral and maxillofacial surgery based on virtual reality. *Expert Rev. Med. Devices* **2018**, *15*, 435–444. [CrossRef] [PubMed]
4. Zulkefli, S.A.; Shaikhani, M.H.; Nasution, A.K.; Wahab, A.A.; Abdul Kadir, M.R.; Ramlee, M.H. Fabrication and Biomechanical Evaluation of Polyurethane Material for Synthetic Bone. *J. Phys. Conf. Ser.* **2019**, *1372*, 012013. [CrossRef]
5. Agrawal, N.; Turner, A.; Grome, L.; Abu-Ghname, A.; Davis, M.J.; Reece, E.M.; Buchanan, E.P.; Winocour, S. Use of Simulation in Plastic Surgery Training. *Plast. Reconstr. Surg. Glob. Open* **2020**, *8*, e2896. [CrossRef] [PubMed]
6. Li, K.H.C.; Kui, C.; Lee, E.K.M.; Ho, C.S.; Wong, S.H.; Wu, W.; Wong, W.T.; Voll, J.; Li, G.; Liu, T.; et al. The role of 3D printing in anatomy education and surgical training: A narrative review. *MedEdPublish* **2017**, *6*, 92. [CrossRef] [PubMed]
7. Oliscovicz, N.F.; Shimano, A.C.; Marcantonio, E., Jr.; Lepri, C.P.; Dos Reis, A.C. Analysis of primary stability of dental implants inserted in different substrates using the pullout test and insertion torque. *Int. J. Dent.* **2013**, *2013*, 194987. [CrossRef] [PubMed]

8. Mehrotra, D.; Markus, A.F. Emerging simulation technologies in global craniofacial surgical training. *J. Oral Biol. Craniofac. Res.* **2021**, *11*, 486–499. [CrossRef] [PubMed]
9. Longfield, E.A.; Brickman, T.M.; Jeyakumar, A. 3D Printed Pediatric Temporal Bone: A Novel Training Model. *Otol. Neurotol.* **2015**, *36*, 793–795. [CrossRef] [PubMed]
10. Alodadi, A. Utilizing Three-dimensional Printing in treating Challenged Dental Implant Cases. *World J. Dent.* **2018**, *9*, 235–241. [CrossRef]
11. Arce, K.; Waris, S.; Alexander, A.E.; Ettinger, K.S. Novel Patient-Specific 3-Dimensional Printed Fixation Tray for Mandibular Reconstruction with Fibular Free Flaps. *J. Oral Maxillofac. Surg.* **2018**, *76*, 2211–2219. [CrossRef] [PubMed]
12. Seifert, L.B.; Schnurr, B.; Herrera-Vizcaino, C.; Begic, A.; Thieringer, F.; Schwarz, F.; Sader, R. 3D-printed patient individualised models vs cadaveric models in an undergraduate oral and maxillofacial surgery curriculum: Comparison of student's perceptions. *Eur. J. Dent. Educ.* **2020**, *24*, 799–806. [CrossRef] [PubMed]
13. Lim, C.G.T.; Campbell, D.I.; Cook, N.; Erasmus, J. A case series of rapid prototyping and intraoperative imaging in orbital reconstruction. *Craniomaxillofac. Trauma Reconstr.* **2015**, *8*, 105–110. [CrossRef] [PubMed]
14. Somji, S.H.; Valladares, A.; Ho Kim, S.; Cheng Paul Yu, Y.; Froum, S.J. The use of 3D models to improve sinus augmentation outcomes—A case report. *Singap. Dent. J.* **2017**, *38*, 63–70. [CrossRef] [PubMed]
15. Sieira Gil, R.; Roig, A.M.; Obispo, C.A.; Morla, A.; Pagès, C.M.; Perez, J.L. Surgical planning and microvascular reconstruction of the mandible with a fibular flap using computer-aided design, rapid prototype modelling, and precontoured titanium reconstruction plates: A prospective study. *Br. J. Oral Maxillofac. Surg.* **2015**, *53*, 49–53. [CrossRef] [PubMed]
16. Jacek, B.; Maciej, P.; Tomasz, P.; Agata, B.; Wiesław, K.; Radosław, W.; Filip, G. 3D printed models in mandibular reconstruction with bony free flaps. *J. Mater. Sci. Mater. Med.* **2018**, *29*, 23. [CrossRef] [PubMed]
17. Jacobo, O.M.; Giachero, V.E.; Hartwig, D.K.; Mantrana, G.A. Three-dimensional printing modeling: Application in maxillofacial and hand fractures and resident training. *Eur. J. Plast. Surg.* **2018**, *41*, 137–146. [CrossRef]
18. Meglioli, M.; Naveau, A.; Macaluso, G.M.; Catros, S. 3D printed bone models in oral and cranio-maxillofacial surgery: A systematic review. *3D Print. Med.* **2020**, *6*, 30. [CrossRef] [PubMed]
19. Sarker, S.K.; Patel, B. Simulation and surgical training. *Int. J. Clin. Pract.* **2007**, *61*, 2120–2125. [CrossRef] [PubMed]
20. Wu, Y.Y.; Rajaraman, M.; Lee, B.; Plakseychuk, A.; Shimada, K. A Patient-Specific Flexible 3D Printed Orthopedic Model for Training and Teaching of Clubfoot Correction Surgery. *3D Print. Addit. Manuf.* **2016**, *3*, 98–105. [CrossRef]
21. Akhoundi, B.; Behravesh, A.H. Effect of Filling Pattern on the Tensile and Flexural Mechanical Properties of FDM 3D Printed Products. *Exp. Mech.* **2019**, *59*, 883–897. [CrossRef]
22. Algarni, M.; Ghazali, S. Comparative Study of the Sensitivity of PLA, ABS, PEEK, and PETG's Mechanical Properties to FDM Printing Process Parameters. *Crystals* **2021**, *11*, 995. [CrossRef]
23. Tajarernmuang, T.; Sawangrat, C.; Jomjunyong, S. Effect of process parameters to flexural strength of 3D printed anatomical bone part. *IOP Conf. Ser. Mater. Sci. Eng.* **2019**, *635*, 012034. [CrossRef]
24. Hanon, M.M.; Zsidai, L.; Ma, Q. Accuracy investigation of 3D printed PLA with various process parameters and different colors. *Mater. Today Proc.* **2021**, *42*, 3089–3096. [CrossRef]
25. Schulze, M.; Gosheger, G.; Bockholt, S.; de Vaal, M.; Budny, T.; Tönnemann, M.; Pützler, J.; Bövingloh, A.S.; Rischen, R.; Hofbauer, V.; et al. Complex Bone Tumors of the Trunk—The Role of 3D Printing and Navigation in Tumor Orthopedics: A Case Series and Review of the Literature. *J. Pers. Med.* **2021**, *11*, 517. [CrossRef] [PubMed]
26. Qamar Tanveer, M.; Mishra, G.; Mishra, S.; Sharma, R. Effect of infill pattern and infill density on mechanical behaviour of FDM 3D printed Parts- acurrent review. *Mater. Today Proc.* **2022**, *62*, 100–108. [CrossRef]
27. Hochman, J.B.; Kraut, J.; Kazmerik, K.; Unger, B.J. Generation of a 3D printed temporal bone model with internal fidelity and validation of the mechanical construct. *Otolaryngol. Head Neck Surg.* **2014**, *150*, 448–454. [CrossRef] [PubMed]
28. Haffner, M.; Quinn, A.; Hsieh, T.; Strong, E.B.; Steele, T. Optimization of 3D Print Material for the Recreation of Patient-Specific Temporal Bone Models. *Ann. Otol. Rhinol. Laryngol.* **2018**, *127*, 338–343. [CrossRef] [PubMed]
29. McMillan, A.; Kocharyan, A.; Dekker, S.E.; Kikano, E.G.; Garg, A.; Huang, V.W.; Moon, N.; Cooke, M.; Mowry, S.E. Comparison of Materials Used for 3D-Printing Temporal Bone Models to Simulate Surgical Dissection. *Ann. Otol. Rhinol. Laryngol.* **2020**, *129*, 1168–1173. [CrossRef] [PubMed]
30. Wang, X.; Shujaat, S.; Shaheen, E.; Jacobs, R. Quality and haptic feedback of three-dimensionally printed models for simulating dental implant surgery. *J. Prosthet. Dent.* **2024**, *131*, 660–667. [CrossRef] [PubMed]
31. Cafino, R.; Soliven, M.M.T.; Velasco, L.C.; Lopez, K.H. Evaluation of polyethylene terephthalate glycol (PETG), Simubone™, and photopolymer resin as 3D printed temporal bone models for surgical simulation. *Asian J. Surg.* **2024**, *47*, 237–244. [CrossRef] [PubMed]
32. Benca, E.; Eckhart, B.; Stoegner, A.; Unger, E.; Bittner-Frank, M.; Strassl, A.; Gahleitner, C.; Hirtler, L.; Windhager, R.; Hobusch, G.M.; et al. Dimensional accuracy and precision and surgeon perception of additively manufactured bone models: Effect of manufacturing technology and part orientation. *3D Print. Med.* **2024**, *10*, 5. [CrossRef] [PubMed]

33. Requena-Pérez, M.V.; Andrés-Cano, P.; Galán-Romero, L.; Suffo, M. Comparative study of biomodels manufactured using 3D printing techniques for surgical planning and medical training. *Expert Rev. Med. Devices* **2024**, *21*, 239–248. [CrossRef] [PubMed]
34. Weinschenk, R.C.; Oldham, B.M.; Nagaraja, K.M.; Alam, F.; Samade, R.; Li, W. Three-dimensional-printed femoral diaphysis for biomechanical testing-Optimization and validation. *J. Orthop. Res.* **2024**, *42*, 2735–2742. [CrossRef] [PubMed]
35. Wojnowski, W.; Marć, M.; Kalinowska, K.; Kosmela, P.; Zabiegała, B. Emission Profiles of Volatiles during 3D Printing with ABS, ASA, Nylon, and PETG Polymer Filaments. *Molecules* **2022**, *27*, 3814. [CrossRef] [PubMed]
36. Nagy, Á.L.; Tóth, Z.; Tarjányi, T.; Práger, N.T.; Baráth, Z.L. Biomechanical properties of the bone during implant placement. *BMC Oral Health* **2021**, *21*, 86. [CrossRef] [PubMed]
37. *ISO 178:2019*; Plastics—Determination of Flexural Properties. International Organization for Standardization: Geneva, Switzerland, 2019.
38. Bauer, M.K. Vergleich der Biomechanik Herkömmlicher Chirurgischer Methoden zur Versorgung von Rippenfrakturen mit dem Neuen Bioresorbierbaren Implantat Bio—ISOS. Doctor's Dissertation, Ludwig-Maximilians-Universität München, München, Germany, 2012. [CrossRef]
39. Lee, W.-J.; Kim, Y.H.; Hong, S.-D.; Rho, T.-H.; Kim, Y.H.; Dho, Y.-S.; Hong, C.-K.; Kong, D.-S. Development of 3-dimensional printed simulation surgical training models for endoscopic endonasal and transorbital surgery. *Front. Oncol.* **2022**, *12*, 966051. [CrossRef] [PubMed]
40. Schlegel, L.; Ho, M.; Fields, J.M.; Backlund, E.; Pugliese, R.; Shine, K.M. Standardizing evaluation of patient-specific 3D printed models in surgical planning: Development of a cross-disciplinary survey tool for physician and trainee feedback. *BMC Med. Educ.* **2022**, *22*, 614. [CrossRef] [PubMed]
41. American College of Radiology. 3D Printing Data Dictionary. Available online: https://nrdrsupport.acr.org/support/solutions/articles/11000073770 (accessed on 20 October 2024).
42. Vercellotti, T. Technological characteristics and clinical indications of piezoelectric bone surgery. *Minerva Stomatol.* **2004**, *53*, 207–214. [PubMed]
43. Spencer, J. Patients in health professional education: So much known, so much yet to understand. *Med. Educ.* **2010**, *44*, 9–11. [CrossRef] [PubMed]
44. Werz, S.M.; Zeichner, S.J.; Berg, B.-I.; Zeilhofer, H.-F.; Thieringer, F. 3D Printed Surgical Simulation Models as educational tool by maxillofacial surgeons. *Eur. J. Dent. Educ.* **2018**, *22*, e500–e505. [CrossRef] [PubMed]
45. Mori, K.; Yamamoto, T.; Nakao, Y.; Esaki, T. Surgical simulation of cerebral revascularization via skull base approaches in the posterior circulation using three-dimensional skull model with artificial brain and blood vessels. *Neurol. Med. Chir.* **2011**, *51*, 93–96. [CrossRef] [PubMed]
46. Unger, B.J.; Kraut, J.; Rhodes, C.; Hochman, J. Design and Validation of 3D Printed Complex Bone Models with Internal Anatomic Fidelity for Surgical Training and Rehearsal. *Stud. Health Technol. Inform.* **2014**, *196*, 439–445. [CrossRef]
47. Cohen, J.; Reyes, S.A. Creation of a 3D printed temporal bone model from clinical CT data. *Am. J. Otolaryngol.* **2015**, *36*, 619–624. [CrossRef] [PubMed]
48. Rose, A.S.; Kimbell, J.S.; Webster, C.E.; Harrysson, O.L.A.; Formeister, E.J.; Buchman, C.A. Multi-material 3D Models for Temporal Bone Surgical Simulation. *Ann. Otol. Rhinol. Laryngol.* **2015**, *124*, 528–536. [CrossRef] [PubMed]
49. Probst, R.; Stump, R.; Mokosch, M.; Röösli, C. Evaluation of an Infant Temporal-Bone Model as Training Tool. *Otol. Neurotol.* **2018**, *39*, e448–e452. [CrossRef] [PubMed]
50. Rashad, A.; Sadr-Eshkevari, P.; Heiland, M.; Smeets, R.; Prochnow, N.; Hoffmann, E.; Maurer, P. Practitioner experience with sonic osteotomy compared to bur and ultrasonic saw: A pilot in vitro study. *Int. J. Oral Maxillofac. Surg.* **2015**, *44*, 203–208. [CrossRef] [PubMed]


**Disclaimer/Publisher's Note:** The statements, opinions and data contained in all publications are solely those of the individual author(s) and contributor(s) and not of MDPI and/or the editor(s). MDPI and/or the editor(s) disclaim responsibility for any injury to people or property resulting from any ideas, methods, instructions or products referred to in the content.